Supplemental Document

Optics EXPRESS

Single photon imaging and sensing of highly obscured objects around the corner: supplement

SHENYU ZHU,[1,2] YONG MENG SUA,[1,2,3] PATRICK REHAIN,[1,2] AND YU-PING HUANG[1,2,4]

[1]*Department of Physics, Stevens Institute of Technology, 1 Castle Point Terrace, Hoboken, New Jersey 07030, USA*
[2]*Center for Quantum Science and Engineering, Stevens Institute of Technology, 1 Castle Point Terrace, Hoboken, New Jersey 07030, USA*
[3]*sua@stevens.edu*
[4]*yuping.huang@stevens.edu*

Supplement DOI: https://doi.org/10.6084/m9.figshare.16974262

Parent Article DOI: https://doi.org/10.1364/OE.441764

Single photon imaging and sensing of highly obscured objects around the corner: supplemental document

1. NON-LINE-OF-SIGHT SURFACE NORMAL RETRIEVAL

In the non-line-of-sight(NLOS) positioning experiment of the bars, the first returning signal peak in the time-histogram is picked as the first-arrival signal photons from the object. Although the width of the bars are less than the spatial resolution of the system, the time of flight is still different for the two edges of the bar. Considering the geometry of the setup as Fig. S1 b shows, the time of flight uncertainty on the i^{th} scanning point for the j^{th} bar can be interpreted as $ds = |\overline{O_iA_j} - \overline{O_iB_j}| = \sqrt{\overline{O_iP_j}^2 + (\frac{\overline{A_jB_j}}{2})^2 - \cos\angle O_iP_jA_j \cdot \overline{A_jB_j} \cdot \overline{O_iP_j}} - \sqrt{\overline{O_iP_j}^2 + (\frac{\overline{A_jB_j}}{2})^2 + \cos\angle O_iP_jA_j \cdot \overline{A_jB_j} \cdot \overline{O_iP_j}}$, where $\overline{A_jB_j}$ is the bar width (about 5mm), and $\overline{O_iP_j}$ is the distance from the scanning point to the midle point of the bar (about 12 cm). The complementary of the tilt angle, $\angle O_iP_jA_j$, is different at each scanning points. In the experiment, the two bars were facing at the center of the wall, such that the largest tilt angle is about 12° ($\angle O_iP_jA_j$ about 78°), which corresponds to $ds_{max} \approx 1mm$ or $6.7ps$ temporal difference.

We used a simple least square approximation for the bar positioning, which does not assume a specific shape of the surface. So the largest error of one scanning point can be $\Delta t = \sqrt{10^2 + 6.7^2} \approx 12ps$. By increasing the number of pixels N which is 16 in current experiment, we can decrease the standard deviation of the result by $\sqrt{N}$, which is shown as the very narrow depth distribution in the positioning result.

This time-of-flight sensitivity of NGSPD provides the potential of evaluating the normal of the hidden surface[1] just using the time-of-flight of the first-arrival photons. A 1.2-cm width bar (wider than the spatial resolution) taped with retroreflector is used as the object, and is put onto a rotational stage in front of the diffuser. First, its surface normal is adjusted to be parallel to the surface normal of the diffuser, which is labelled as 0°. Then the bar is yawed using the rotational stage. We measure the time-resolved histogram of the bar on a row of scanning points, at each of the three yaw angles($-10°$, 0° and 10°). The earliest returning peak on the time-resolved histogram is chosen and plotted for each scanning point as shown in the last row in Fig.S2. The simulation results of the first returning photons' arrival time are plotted together, which shows promising consistency comparing with the experiment results. Thus the travel time of the first returning photons reveals the surface normal of the object. The resolving algorithm for normal angle evaluation needs to be developed in further steps.

2. ADDITIONAL FIGURES

For NLOS positioning and acoustic sensing experiments, we used the setup shown in Fig. S3. In the NLOS positioning experiment, the probe laser beam scans a horizontal row of points on the diffuser, while no cellphone actuation is added. In the acoustic sensing experiment, the probe laser beam locates on one point on the diffuser, while the two cellphones play different frequencies actuating each object.

REFERENCES

1. S. I. Young, D. B. Lindell, B. Girod, D. Taubman, and G. Wetzstein, "Non-line-of-sight surface reconstruction using the directional light-cone transform," in *Proc. CVPR*, (2020).

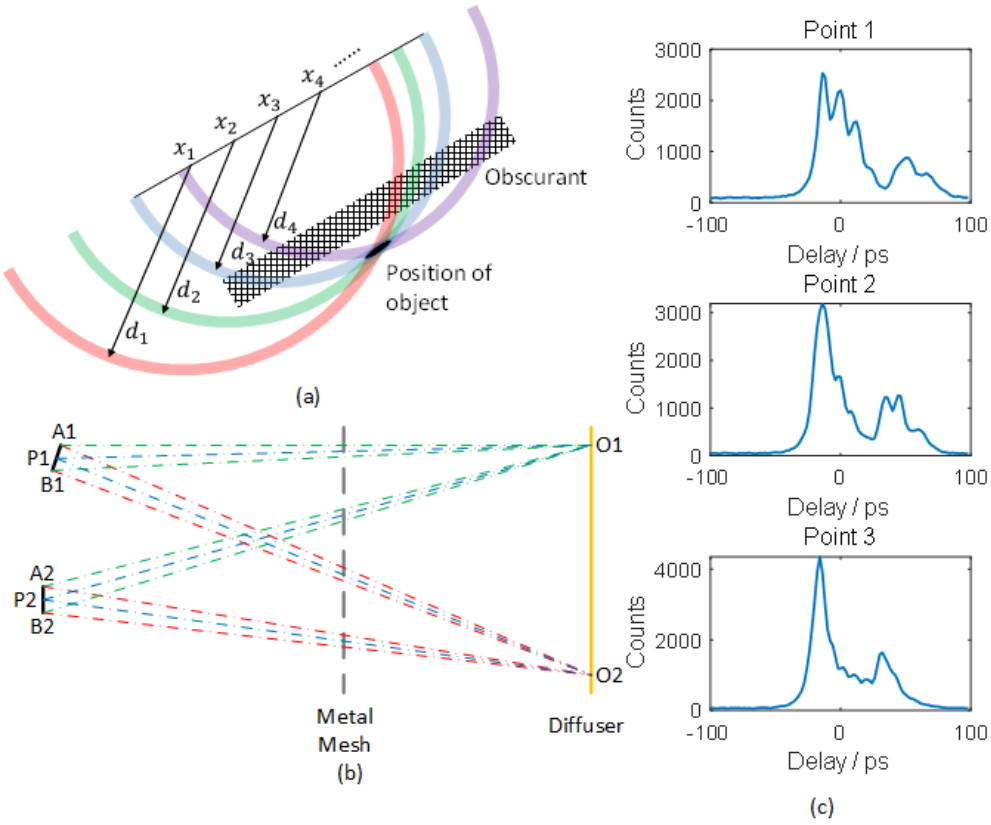

Fig. S1. NLOS positioning. (a) depicts the spherical probability distribution of the NLOS positioning experiment. The time-resolved measurement at each scanning point x_i provides a distance d_i to the object. (b) shows the geometric of the positioning, O1 and O2 are the scanning points on the diffuser, A1B1 and A2B2 are the bars. (c) is the scanning raw data of the two bars. When scanning point shifts, the time-of-flight of the back-scattered photons from the two bars varies. We simply picked the first peak of the two responses for processing.

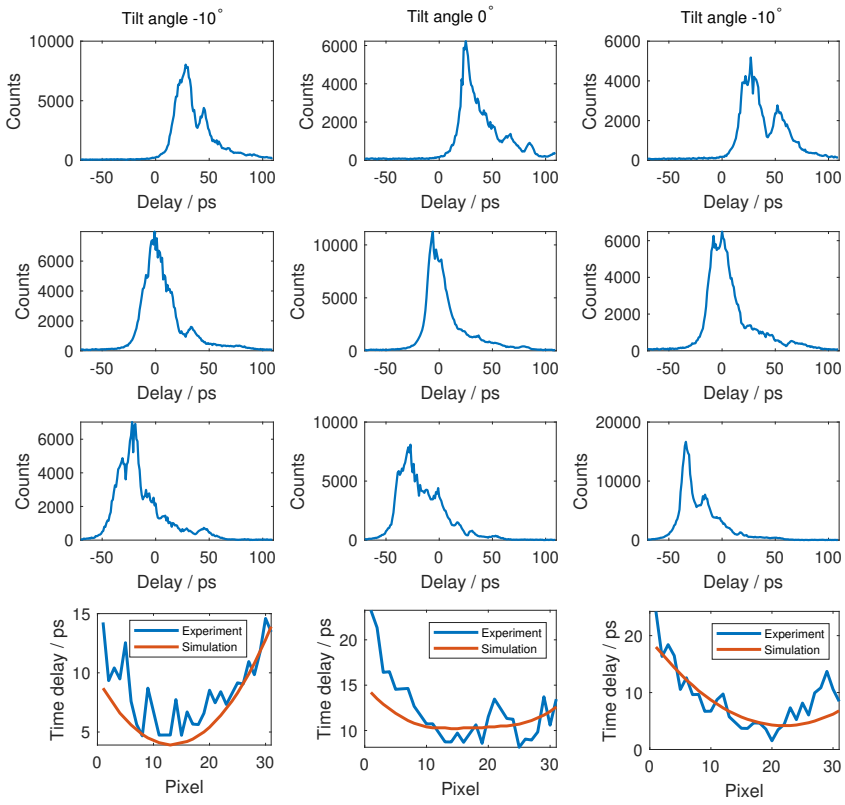

Fig. S2. NLOS time-of-flight measurement for different surface normal aiming at -10°, 0° and 10°. The first three rows of plotting are original data, each row corresponds to one pixel and each column corresponds to one tilt angle. At each pixel, we pick the time of the earliest arriving signal peak, and compare with the simulation result at the same scanning points, which are plotted in the last row. For the pixels on the edge, the error from the experiment and simulation differs most, which can be brought in by the fact that the intensity from the edge is lower than other parts, then the real earliest peak can be immersed.

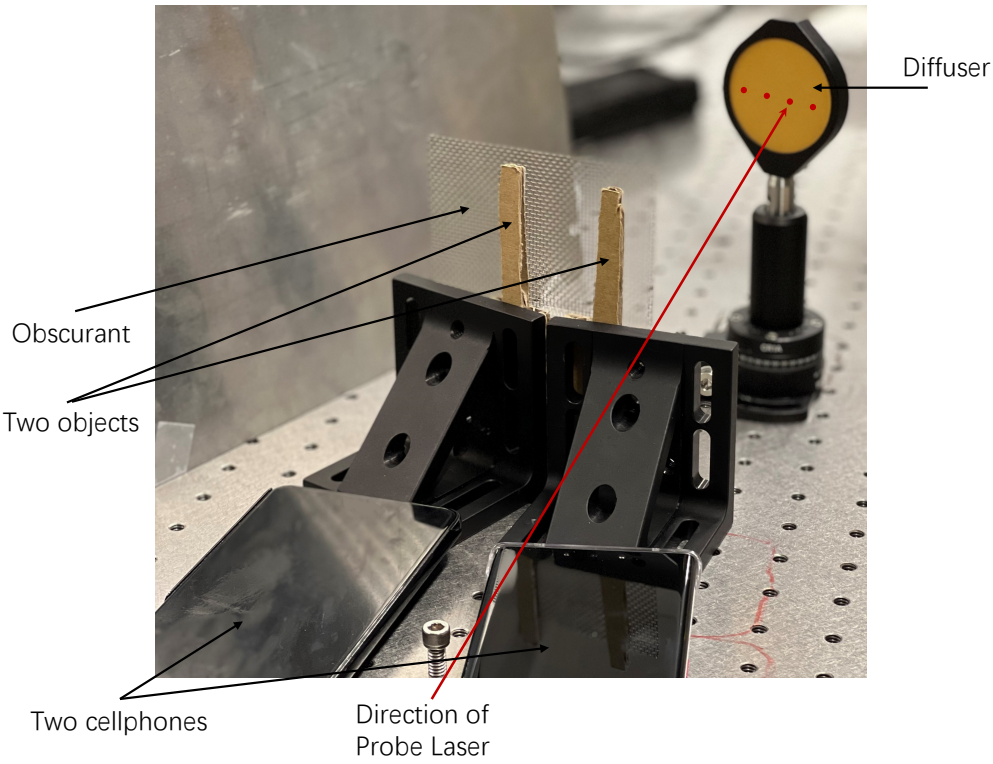

Fig. S3. NLOS setup for positioning and acoustic sensing. Red dots labeled on the diffuser indicates the row of scanning points for NLOS positioning.